Efficient fabrication of Ti6Al4V alloy by means of multi-laser beam selective laser melting

Fangzhi Li*, Zemin Wang* and Xiaoyan Zeng*

* Huazhong University of Science and Technology, Wuhan 430074, PR China

Abstract

A self-developed four-laser beam selective laser melting (SLM) system was used to fabricate Ti6Al4V alloy samples in this study. The relative density, micro-hardness and mechanical properties of all isolated processing areas were compared under optimized processing parameters to ensure the consistency of this system. Microstructures in overlap areas are dominated by columnar grains along the building direction and matensitic needles α′ inclined at about ± 45° to the building direction, which are similar with those in isolated areas. Mechanical properties in overlap areas are also not inferior to those in isolated areas. The results prove the feasibility to fabricate large-scale components with a uniform microstructure and mechanical property by this SLM system. By the use of four lasers, this system can provide a high building rate of 80 cm^3/h.

Keywords

Multi-laser beam; Selective laser melting; Ti6Al4V; Microstructure; Mechanical property;

Introduction

Laser additional manufacturing (LAM) has roused extensive attention for its capability to build up complex three dimensional features in an additive way. This process uses 3D CAD data as a digital information source to create three-dimensional metal components through fusing fine metal powders by a focused high-power laser beam layer by layer. Through this process, direct energy deposition or powder bed fusion are commonly used for manufacturing metallic materials. In the past few decades, researchers mainly focused on relative density, microstructures, surface properties and mechanical properties, etc. of different kinds of materials, size and shapes of metal components. Benefit by their research, LAM process was widely available in the field of aerospace, die forming and medical implants, etc., being as an effective complement of traditional processing methods like casting, forging and welding.

However, the state-of-the-art process is not fully competent to series production for the demand of large-scale components and the restriction of fabrication efficiency. In order to improve this efficiency, it is indispensable to increase the build rate significantly by matching a thicker powder layer with a higher scanning velocity under higher laser power[1].

Laser cladding deposition (LCD), also referred to as direct laser deposition (DLD), laser melting deposition (LMD) or Laser-Engineered Net Shaping (LENS), which belongs to the direct energy deposition category, showed a great potential to form large scale components efficiently for its natural high laser power and mm-scale laser beam diameter. During this process, metal powder is injected into the melting pool to be melt and then solidified in a sudden

time onto a substrate. Tian[2] et al., achieved a powder delivery rate of 100 cm^3/h Ti-4Al-1.5Mn titanium alloy by the use of a 5 kW CO_2 laser with a laser beam diameter of 5 mm. Zhu[3] et al., further increase the powder delivery rate to 600-1000 g/h of Ti-6.5Al-3.5Mo-1.5Zr-0.3Si titanium alloy by a 8 kW CO_2 laser. Yu[4] et al., obtained Ti6Al4V part with relative density up to 99.8% by the use of a 7 kW IPG fiber laser with spot size of 1.2 mm. Qiu[5] et al., successfully fabricated large Ti6Al4V structures by the use of a 4 kW disc laser and an automatic spot change collimator (from 0.2 to 6 mm). Their research demonstrate the capability of LCD process to fabricate large scale titanium structures efficiently. Due to these characteristics, LCD process has been presented a rapid expansion in aerospace field. On the other hand, large laser spot size and powder layer thickness will inevitably lead to poor shape precision together with the factor of direct energy deposition category. Therefore, LCD is still hard to meet the requirements of components with high precision and complex structure.

Compared with LCD, selective laser melting (SLM), which belongs to the powder bed fusion category, is more suitable for precision forming of complex components with the aid of support structures and pre-paved powders. However, current SLM technology usually contains laser power no more than 500 W and powder thickness of 20-60 μm[6][7]. The related low building rate obviously cannot meet the demand of large scale components. In order to improve this efficiency, a kW-level laser was first integrated into a SLM system by Schleifenbaum[8] et al., together with a new multi-beam to maintain accuracy and detail resolution of manufactured components. With this SLM system, Buchbinder[9] et al., increase the build rate to approx. 75.6 cm^3/h for the production of AlSi10Mg parts while reaching densities above 99.5%. Ma[1] et al., further increase laser power to 6kW which can supply a sufficient energy density to obtain near-full-density part while maximum layer thickness reach to 150 μm of 1Cr18Ni9Ti stainless steel. The development of high power (HP) SLM provides a greater build rate than traditional SLM and a higher fabrication accuracy than LCD. However, limited by machining dimension, HP SLM is not capable to fabricate components in large scale size (usually limited in 250 mm × 250 mm).

LCD and HP SLM both based on high power laser and its related large beam diameter and higher layer thickness, which in turn lead to restriction of poor accuracy in a certain extent. In order to combine the advantage of high precision of traditional SLM process and high efficiency of high power LAM process, a multi-laser beam SLM system is developed. This system contains a multi-beam system including 4 independent continuous wave IPG YLR-500 fiber lasers together with 4 optical systems. In this multi-beam system, four lasers are in action simultaneously, providing four times the build rate compared with single laser SLM system while obtaining considerable accuracy. Meanwhile, this system can achieve a build envelope of 500 × 500 × 530 mm^3. In the previous attempt, components has a great deal of cracking tendency at slicing line when overlap width is 0 for the lack of fusion. In order to overcome this shortage, overlap width from 0.5 to 2.5 mm was introduced in the experiments. In this situation, overlap area will go through another thermal cycle due to the re-melting of adjacent multi-beams.

There is no doubt that the multi-beam SLM system can provide higher processing efficiency and the ability to process larger scale of components. However, the experience of fabrication by multi-beam SLM system is not been reported yet. The formability of this kind of system still remains to be verified.

In this paper, detailed investigation on the effects of overlap area between adjacent processing areas of Ti6Al4V titanium alloy by multi-beam SLM system was studied. The microstructure and mechanical properties of the fabricated samples in both isolated region and overlap area were compared.

Self-developed multi-laser beam SLM system

A self-developed multi-beam SLM system (NRD-SLM-500) was used to process Ti6Al4V titanium alloy. This system mainly consisted of four continuous wave IPG YLR-500 fiber lasers (λ=1.07 μm, maximum output power of 500 W, 100 μm spot size), four matrix-arranged scanning galvanometers (scanned area of 250 mm in both length and width), a building platform and a powder providing system, shown in Fig.1(a). By combining these matrix-arranged scanning galvanometers, four lasers can work together to build one big part or work separately to build several parts within 500(L)×500(W)×530(H) mm^3. Compared with SLM systems with single laser beam, NRD-SLM-500 has two functions: larger build envelope size and higher build rate.

The build rate can be improved by three methods: the use of four lasers, double-direction powder delivery method and segmented powder delivery strategy, shown in Fig.1 (b).

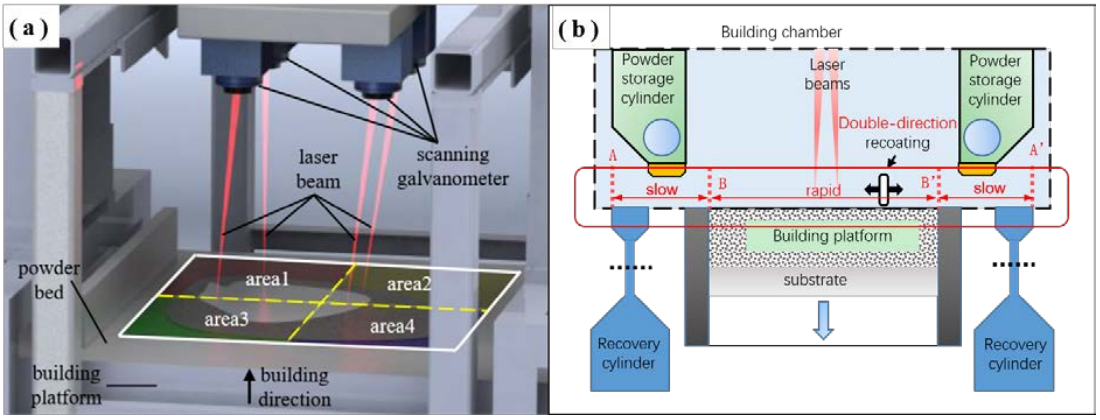

Fig. 1 Schematic diagram of NRD-SLM-500 system used in this study

The manufacturing process can be decomposed as following steps shown in Fig.2: part design-file import-slicing and segmentation into four parts-fabricating. By the use of four lasers, this system can provide a high build rate of 80 cm^3/h (considering the time of powder delivery).

Experimental details

Gas atomized Ti6Al4V powders with an average particle size below 50 μm were used as the starting material, whose morphology is shown in Fig.3. Meanwhile, the chemical composition and particle size distribution were listed in Table 1. Based on the standard alternating x/y scanning strategy[10], relative hatch angle of scanning directions in adjacent scanning areas should be took into account. The sampling position, scanning strategy and configuration of tensile samples built in isolate and overlap area were shown in Fig.4 (a)-(c), respectively. In order to overcome the cracking tendency at slicing ling, overlap width from 0.5 to 2.5 mm was invested in the experiments.

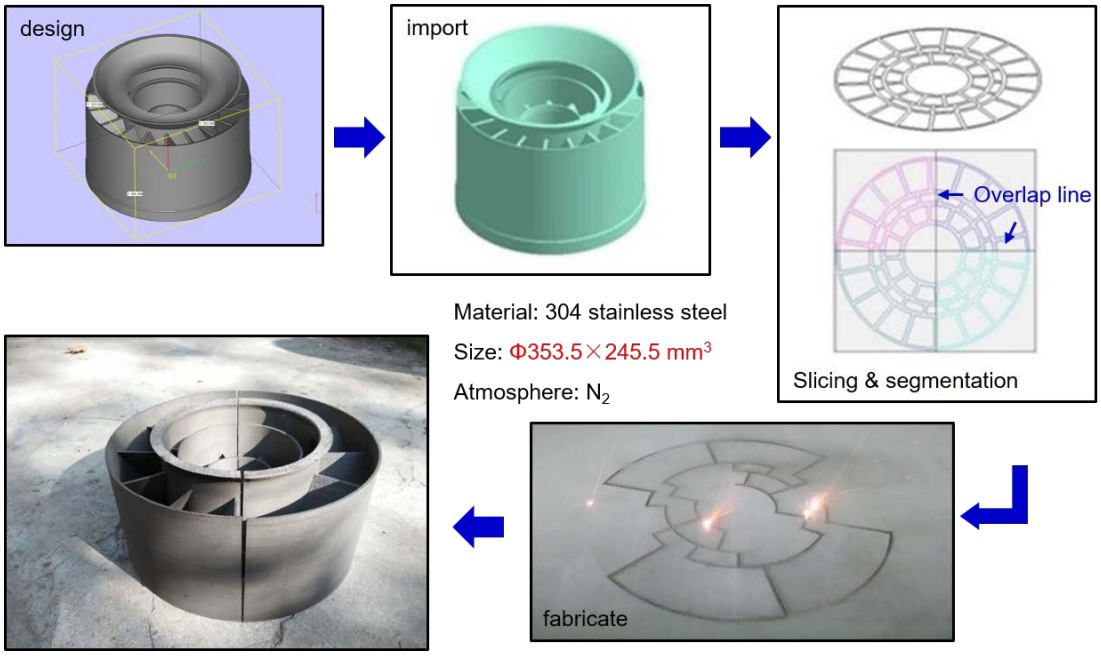

Fig. 2 Manufacturing process of multi-laser beam SLM system

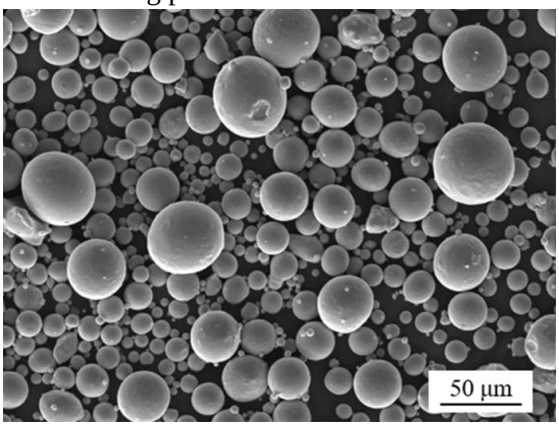

Fig. 3 Characteristic morphology of Ti6Al4V powders used in SLM experiments

Table 1 The chemical composition and particle size distribution of Ti6Al4V powders used in SLM process

Chemical composition (W_t%)			Particle size distribution (μm)		
Ti	Al	V	D_v10	D_v50	D_v90
89.77	6.97	3.26	19.0	33.8	57.3

In the initial stage of the experiment, cuboid and tensile samples were built in 4 isolated processing areas to test the consistency. For each processing area corresponds the same types of laser and optical system, sample fabricated in 4 areas can be considered under the same processing conditions. In this paper, samples fabricated in area 3, area 4 and their overlap area were chosen as the research object. The SLM parameters used in this study are presented in Table 2.

Surface morphology and microstructure were observed by a digital microscope (Keyence VHX-1000) and a scanning electron microscope (FEI Nova NanoSEM 450), Vickers hardness

tests were carried out using a HVS-1000 microhardness tester at a load of 9.8 N and a dwelling time of 20 s. Tensile test pieces were designed according to Chinese GB/T 228-2002 standard, as shown in Fig. 3 (a). For a further instruction, tensile test pieces fabricated at overlap area were pre-machined groove structure to test mechanical properties of overlap area. All tensile test pieces were tested using a zwick/roell tester to evaluate the tensile properties at room temperature with a rate of 2 mm/min.

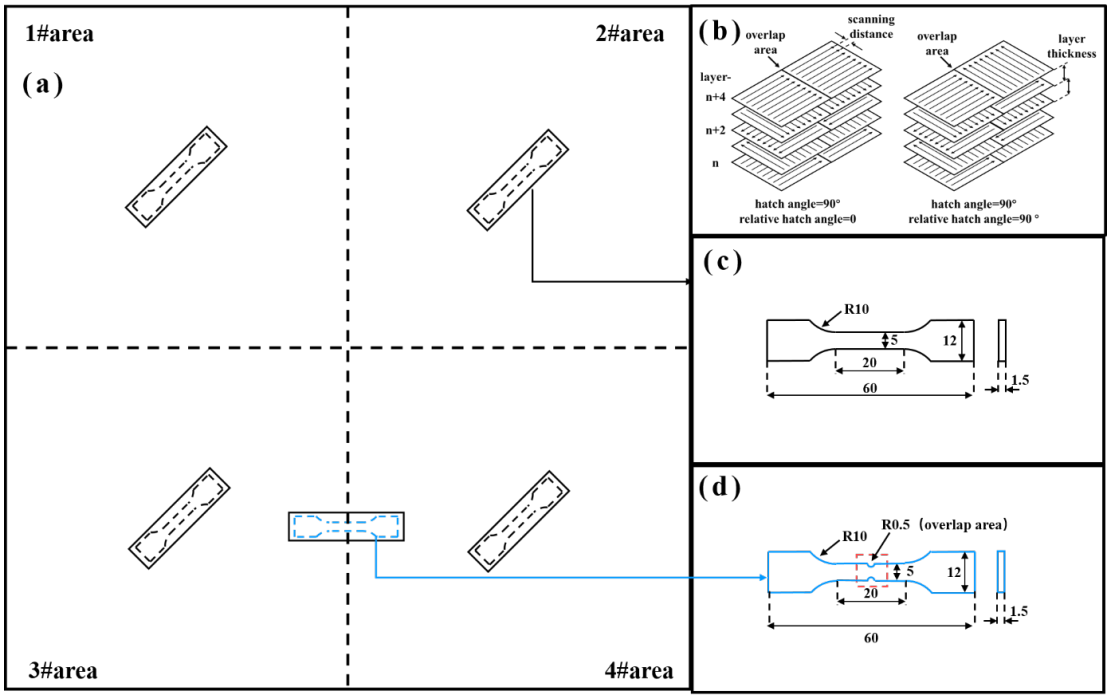

Fig. 4 (a) sampling position and (b) laser scanning strategy, and (c), (d) configuration of tensile samples built in isolate and overlap area

Table 2 SLM manufacturing parameters used in this study

Processing parameters	Values
Laser power (W)	300
Scanning speed (mm/s)	1000
Scanning distance (mm)	0.12
Layer thickness (μm)	40
Hatch angle (°)	90
Relative hatch angle (°)	0, 90
Overlap width (mm)	0.5-2.5

Results and discussions

3.1 Consistency of isolated processing areas

Table 3 lists the relative density, micro-hardness and tensile properties of samples built in 1#-4# processing areas. Under optimized parameter, unique micro-hardness and mechanical properties were obtained at a high building rate of 80 cm^3/h

Table 3 Relative density, micro-hardness and tensile properties of samples built in 1#-4# processing areas

	1# area	2# area	3# area	4# area
Relative density (%)	99.92	99.81	99.84	99.93
Micro-hardness (HV)	408±17	407±16	397±11	411±4
Rm (MPa)	1226±38	1224±15	1224±11	1234±32
Rp0.2 (MPa)	1131±41	1140±11	1151±39	1127±24
El (%)	5.3±0.5	5.2±0.6	5.3±0.6	5.0

3.2 Surface morphology of overlap area

Fig. 5 shows the top surfaces of the samples that were fabricated across overlap area with varied overlap width and relative hatch angle. Fig.5 (a)-(e) represent relative hatch angle of 0 while Fig.5 (f)-(j) represent relative hatch angle of 90°. The white arrows show the scanning direction of final layer. The yellow ones show stair-steps produced in multi-beam SLM process. Apparently, stair-step effect is more serious when relative hatch angle is 0° than 90°. Normally, the stair-step effect will cause nonuniformity of actual powder layer thickness and do harm to SLM process. Fig.5 (k) and (l) show the three-dimensional contours of Fig.5 (b) and (g) for a more intuitive observation. The height of stair-step is only affected by the relative hatch angle but has no effect on overlap distance varied from 0.5 mm to 2.5 mm through the measurement of cross section from digital microscope. Specifically, the height difference decrease from approximate 180 μm to 60 μm by adjusting the relative hatch angle from 0 to 90°.

Comprehensive consideration processing efficiency and convenience of study, overlap width of 1 mm and relative hatch angle of 90° were adopted in the following studies.

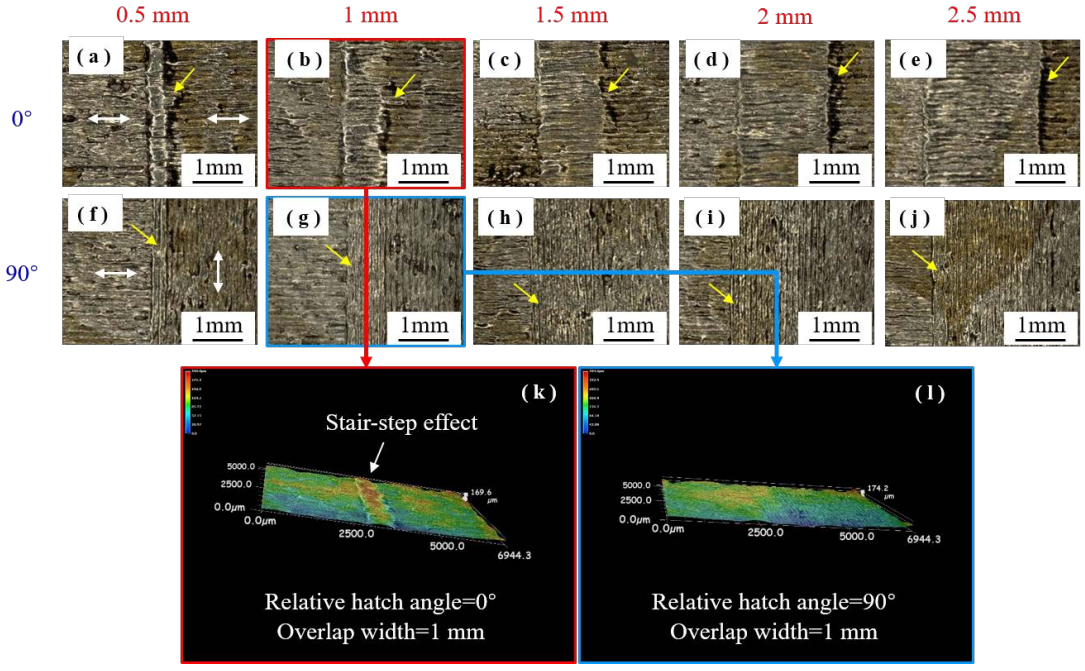

Fig. 5 Surface morphology of overlap area

3.3 Microstructure and mechanical performance of multi-beam

Fig.6 shows the microstructure of samples built in 3#area, 4#area and overlap area. It can be seen from Fig.6 (a)-(c) that all built samples are dominated by columnar grains which tend to elonate along the building direction (i.e. Z direction). All these columnar grains grow over several layers and reach to mm-scale in length with the width of more or less 200 μm. Within the columnar grains, matensitic needles α′ are observed for the fast melting-solidification process. Due to the fast cooling, the β phases transform to α′ phase according to Burgers relation given by Equatation(1)[11]. These matensitic needles show an obvious herringbone distribution and inclined at about ± 45° to the building direction, indicated by blue slashes. This incline is because of a specific Burgers relation between α/α′ phase and β phase which dictates the α′ growth orientation during fast melting-solidification process in SLM fabrication.

$$(1\,1\,0)_{\beta} \leftrightarrow (0\,0\,0\,1)_{\alpha} \tag{1}$$

$$<1\,\bar{1}\,1>_{\beta} \leftrightarrow <1\,1\,\bar{2}\,0>_{\alpha}$$

Fig.(d)-(f) show the horizental section of samples built in 3#area, 4#area and overlap area, respectively. Chessborad patterns of spacing about 120 μm indicated by white dotted box can be observed for the reason of 90° hatch angle betweem adjacent layers in both 3# area, 4# area and overlap area. The spacing width corresponding to the scanning distance used in the experiment.

Comprehensive consideration of both vertical and horizental sections, metallographic structure and distribution in overlap area have no significant difference of the superposition of heat resource by the introduced laser beam compared with 3# and 4# area.

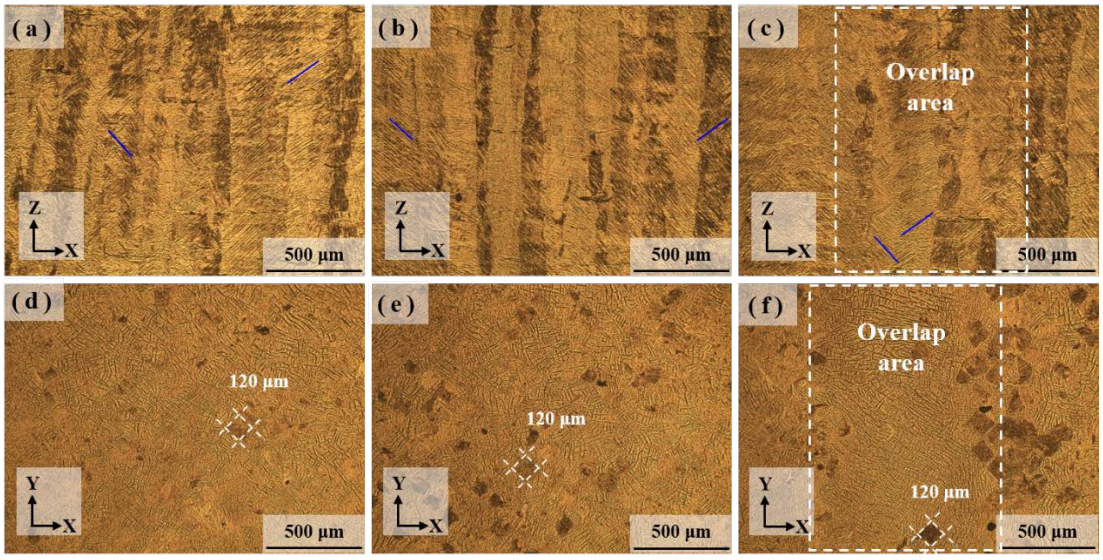

Fig. 6 Microstructure of (a)-(c) vertical section and (d)-(f) horizontal section of samples built in 3#area, 4#area and overlap area, respectively.

Fig.7 (a) shows results for Ti-6Al-4V powder, as-fabricated samples built in 3# area and overlap area. It can be seen that both powders and built samples show the hcp-Ti characteristics

of crystallography. This suggests that neither process of fabrication in isolated area nor re-melting in overlap area contains α/α′→β transformation. However, a slight shift in the hcp-Ti phase peaks to larger 2θ angles was observed, which may be by the reason of the solute redistribution, shown in Fig.7 (b).

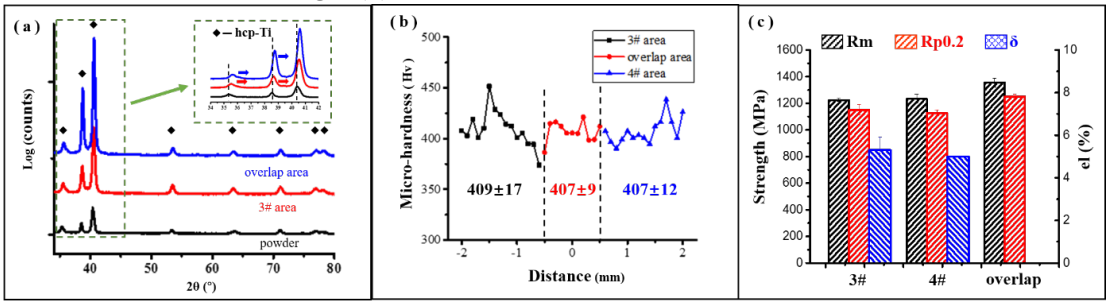

Fig. 7 (a) XRD result for Ti6Al4V powders, as-fabricated samples built in 3# area and overlap area, the green dotted box shows detailed information of 2θ from 34°-42°, (b) micro-hardness of overlap area and its adjacent processing areas and (c) mechanical properties in overlap area compared with isolated areas.

3.4 Fabrication of large scale of component by multi-laser beam SLM

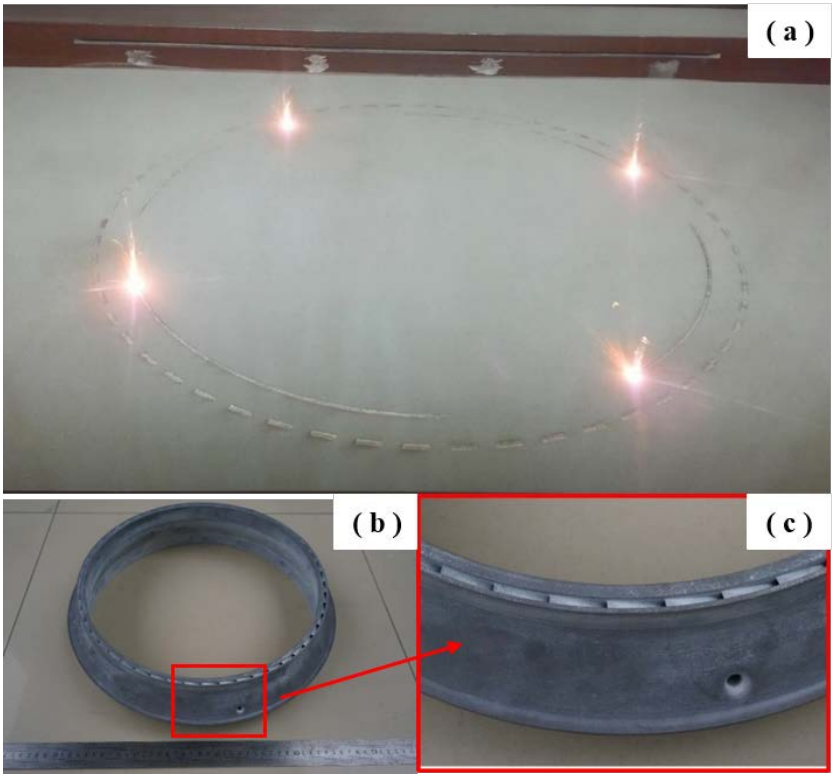

Fig. 8 large scale of component fabricated by multi-laser beam SLM system. (a) fabrication process, (b) real figure of built component and (c) detailed drawing of (b).

Based on the analysis of the above, 4 isolated processing areas and their related overlap areas have the uniform processing ability. This provides the premise to fabricate large scale of component with uniform performances. Fig.8 (a) shows the production process of one Ti6Al4V

model and Fig.13 (b) and (c) show the real figure of this model. Profit from 4 laser beams work at the same time, the multi-laser beam SLM system has an incomparable processing efficiency compared with traditional SLM systems. The largest diameter of this component reach to 401 mm and the height is 93mm.

Conclusion

In this work, cuboid and tensile samples of Ti6Al4V were built in both isolated processing areas and overlap areas. Through the experimental results, samples in 4 isolated areas and overlap areas have uniform microstructure and mechanical properties. Microstructures and mechanical properties of overlap areas are not affected by the relative hatch angle and overlap width. Considering the surface accuracy, θr is adopted in multi-laser beam SLM process. Under the work of 4 laser beams together, a large-scale of component can be fabricated in an efficiency way (build rate up to 80 cm3/h) finally.

Acknowledgements

This work is supported by the National Program on Key Basic Research Project of China (973 Program) under grant (no. 613281), the National Natural Science Foundation of China through program (no. 50905068), and the Fundamental Research Funds for the Central Universities through program (no. HUST: 2016YXZD005).

Reference

[1] Mingming Ma, Zemin Wang, Ming Gao, Xiaoyan Zeng. Layer thickness dependence of performance in high-power selectivelaser melting of 1Cr18Ni9Ti stainless steel. Journal of Materials Processing Technology 215 (2015) 142–150.

[2] X.J. Tian, S.Q. Zhang, A. Li, H.M. Wang. Effect of annealing temperature on the notch impact toughness of a laser melting deposited titanium alloy Ti–4Al–1.5Mn. Materials Science and Engineering A 527 (2010) 1821–1827.

[3] Yanyan Zhu, Xiangjun Tian, Jia Li, Huaming Wang. Microstructure evolution and layer bands of laser melting deposition Ti–6.5Al–3.5Mo–1.5Zr–0.3Si titanium alloy. Journal of Alloys and Compounds 616 (2014) 468–474.

[4] Jun Yu, Marleen Rombouts, Gert Maes, Filip Motmans. Material properties of Ti6Al4V parts produced by laser metal deposition. Physics Procedia 39 (2012) 416-424.

[5] Chunlei Qiu, G.A. Ravi, Chris Dance, Andrew Ranson, Steve Dilworth, Moataz M. Attallah. Fabrication of large Ti–6Al–4V structures by direct laser deposition. Journal of Alloys and Compounds 629 (2015) 351–361

[6] H. Attar, K.G. Prashanth, A.K. Chaubey, M. Calin, L.C. Zhang, S. Scudino, J. Eckert. Mater Lett, 142(2015), pp. 38-41

[7] Xuetong Sun, Huaishu Lin, Xianshuai Chen, Peng Zhang. Mater Lett, 192(2017) , pp. 92-95

[8] H. Schleifenbaum, W. Meiners, K. Wissenbach, C. Hinke. Individualized production by means of high power Selective Laser Melting. CIRP Journal of Manufacturing Science and

Technology 2 (2010) 161–169

[9] Buchbinder, D., Schleifenbaum, H., Heidrich, S., Meiners, W., Bültmann, J. High Power Selective Laser Melting (HP SLM) of Aluminum Parts. Physics Procedia 12 (2011) 271–278

[10] Wang, Z., Guan, K., Gao, M., Li, X., Chen, X., Zeng, X. The microstructure and mechanical properties of deposited-IN718 by selective laser melting. J. AlloysCompd. 2012. 513, 518–520.

[11] Lore Thijs, Frederik Verhaeghe, Tom Craeghs, Jan Van Humbeeck, Jean-Pierre Kruth. A study of the microstructural evolution during selective laser melting of Ti–6Al–4V. Acta Materialia. Volume 58, Issue 9, May 2010, Pages 3303–3312